Published online January 10, 2019



# Evapotranspiration from Corn, Soybean, and Prairie Grasses using the METRIC Model

Nathaniel W. Baeumler, Jeppe Kjaersgaard, and Satish C. Gupta*

## ABSTRACT

Land use in the US Upper Midwest has evolved from small grains and prairie systems to corn (*Zea mays* L.) and soybean [*Glycine max* (L.) Merr.]. This change has been assumed to cause a dramatic decrease in landscape evapotranspiration (ET) and consequently a large increase in streamflow. This study assessed ET from corn, soybean, and native prairie grasses using the satellite image based surface-energy balance model named METRIC in west-central Minnesota. The METRIC model uses properties of satellite images along with daily weather to calculate landscape ET. The land covers analyzed were irrigated and non-irrigated corn, non-irrigated soybean, native prairie grasses under different grazing and burn regimes, and wetlands. For 8 June through 22 Oct. 2015, estimated ET followed the trend: wetlands (717 mm) > non-irrigated corn (662 mm) > irrigated corn (647 mm) > non-irrigated soybean (554 mm) > previously burned prairie (537 mm) > recently burned prairie (406 mm). For 1 May to 22 Oct. 2015, the estimated ET of wetlands, previously burned and recently burned prairie grasses were 884, 666, and 511 mm, respectively. These model estimates showed that ET of native prairie grasses are similar to slightly higher than that of corn and soybean. Considering soybean also replaced low ET small grains suggests that changes in landscape ET from a changeover of vegetative cover starting in 1940s are likely minimal. This supports our earlier findings that recently increased streamflows in the Upper Midwest are primarily from increased precipitation and not due to land cover changes.

## Core Ideas

- Evapotranspiration of native prairie grasses is marginally higher than that of corn and soybean.
- Evapotranspiration of recently burned prairie was lower than those of previously burned prairie.
- Landscape evapotranspiration is likely similar from the changeover of small grains and native prairies to soybean.

Published in Agron. J. 111:1–11 (2019)
doi:10.2134/agronj2018.08.0506
Supplemental material available online



Streamflows in the Mississippi River Basin have been increasing over time, most notably since the mid-1970s. There is an intense debate in the literature as to the reasons for this increase. Some investigators believe it is mainly the result of land use land cover changes including increased subsurface (tile) drainage, cultivation of prairies, and adoption of soybean [*Glycine max* (L.) Merr.] in the modern cropping system (Zhang and Schilling, 2006; Schilling et al., 2010; Wang and Hejazi, 2011; Xu et al., 2013). Others believe it is caused by increased precipitation due to climate change (Karl and Knight, 1998; Lins and Slack, 1999; Novotny and Stefan, 2007; Hoogestraat and Stamm, 2015; Gupta et al., 2015, 2018). The emphasis on soybean is because soybean displaced small grains and prairie systems in the Upper Midwestern United States starting in early 1940s.

The underlying argument for land cover changes as the main driver of increased streamflow in the Upper Midwest is that the prairie systems are perennial and start growing early in the spring. Similarly, small grains are planted in late fall or early spring, thus providing more biomass for higher evaporative demand earlier in the growing season. Comparatively, soybean plants are planted in early to mid-May and do not have large evaporative demand until June.

However, there is limited data on evapotranspiration (ET) of prairie grasses relative to corn (*Zea mays* L.) and soybean in the literature. For example, Weaver and Crist (1924) showed that prairie grasses had less evapotranspiration than oat (*Avena sativa* L.) and alfalfa (*Medicago sativa* L.). Weaver (1941) showed that evapotranspiration losses depended on the type of native prairie grasses and water availability and in some cases it could be more than 1000 mm $yr^{-1}$. However, much of the early evapotranspiration data for prairie grasses were obtained with plants grown in small containers, and thus there could be some edge effects leading to inflation of ET estimates. Also, the earlier work on ET of native prairie grasses was not replicated; therefore, there was little statistical accounting of experimental variability in the ET values.

N.W. Baeumler and S.C. Gupta, Dep. of Soil, Water, and Climate, Univ. of Minnesota, 1991 Upper Buford Circle, St. Paul, MN 55108; and J. Kjaersgaard, Fertilizer Non-Point Section, Minnesota Dep. of Agric., 625 Robert Street N, St. Paul, MN 55155. Received 10 Aug. 2018. Accepted 19 Oct. 2018. *Corresponding author (sgupta@umn.edu).

**Abbreviations:** AOI, area of interest; AQP, Appleton Municipal Airport; CRP, Conservation Reserve Program; DOY, day of the year; ET, evapotranspiration; $ET_{inst}$, instantaneous evapotranspiration; $ET_r$, evapotranspiration from a reference crop; ETrF, evapotranspiration as a fraction of ET from a reference crop; $\overline{\text{ETrF}}$, an average value of ETrF; LAI, leaf area index; METRIC, Mapping Evapotranspiration at High Resolution with Internalized Calibration; MNDNR, Minnesota Department of Natural Resources; NDVI, normalized difference vegetation index; ref, reflectance from Landsat bands.

In the 1950s, agronomic trials were run to assess the effects of fertilization and soil moisture on yield and water use by native prairie grasses. In the last 6 yr of a 9-yr trial with application of 0, 34, and 101 kg of nitrogen ha$^{-1}$, Smika et al. (1961) showed that N addition increased moisture withdrawal at all soil depths in native rangeland plots at Mandan, ND. However, there was no difference in moisture withdrawal between the N treatments in the last 3 yr of the trial. The dominant species at the start of the experiment were blue grama [*Boutelous gracilis* (Kunth) Lag. ex Griffiths], western wheatgrass [*Pascopyrum smithii* Rydb. (Love)], needle-and-thread grass (*Stripa comate* Trin. & Rupr.) and threadleaf sedge (*Carex filifolia* Nutt.). In a subsequent study, Smika et al. (1965) showed that fertilized native grasses under high moisture treatment (compared with natural precipitation) produced about three times more forage and used 38 mm more water. For each N treatment (0, 22, 45, 90, and 179 kg N ha$^{-1}$), water use was linearly related to available soil water. Based on the best-fit curves, the maximum water use was about 381 mm at available soil moisture of about 457 mm and fertilizer application rate of 179 kg N ha$^{-1}$. The corresponding maximum water use for 0 and 22 kg N ha$^{-1}$ treatments was about 305 mm. In a similar study, Power (1985) measured the relative differences in dry matter production, root growth, and water use (5 yr only) between various cool-season grasses at three N application rates (0, 45, and 225 kg N ha$^{-1}$) over a 9-yr period (1970–1978) at Mandan, ND. The species compared were western wheatgrass, crested wheatgrass [*Agropyronn desesrtorum* (Fisch. ex Link) Schult.], intermediate wheatgrass [*Elytrigia intermedia* (Host) Nevski], smooth bromegrass (*Bromus inermis* Leyss.), Russian wildrye [*Psathyrostachys juncea* (Fisch.) Nevski], green needlegrass (*Stipa viridula* Trin.), and Garrison creeping foxtail (*Alopecurus arundinaceus* Poir.). For all species, dry matter production doubled with the addition of 45 kg N ha$^{-1}$. Comparatively, addition of 225 kg N ha$^{-1}$ increased production by three- to fourfold. Intermediate wheatgrass had the highest production, whereas smooth bromegrass, western wheatgrass, and crested wheatgrass had 85 to 90%, and the remaining species 60 to 72% of the production of intermediate wheatgrass. Water use increased by 20 mm in fertilized plots, except in the drought year (1977). In normal years, annual water use varied from 236 to 399 mm for all the above prairie grasses. In 1977, a dry year, water use for the above species varied between 129 and 154 mm. Five-year average water-use and water-use efficiency for the six species varied from 272 to 304 mm and 3.2 to 22.6 kg mm$^{-1}$, respectively.

In comparing the N losses from continuous corn (C-C), corn–soybean (C-S), soybean–corn (S-C), alfalfa and Conservation Reserve Program (CRP) treatments at Lamberton, MN, Randall et al. (1997) showed that drainage losses from perennial crops of alfalfa and CRP were less than that from the row crops of corn and soybean. The study period in Randall et al. (1997) included two very dry (1988, 1989) and one very wet year (1993). For a normal year of 1992, drainage losses followed the trend: CRP (510 mm) > C-S (489 mm) > S-C (478 mm) > C-C (441 mm) > alfalfa (321 mm). In a subsequent publication, these authors reported a 5-yr (1989–1993) average ET of 531, 523, 531, 591, and 552 mm for C-C, C-S, S-C, alfalfa, and CRP, respectively (Huggins et al., 2001). These estimates are similar to the estimates reported by Gupta et al. (2015) for the above treatments. Huggins et al. (2001) also showed that there was some effect of soil-stored water on water losses through tile drainage in subsequent years. They showed that there was a unique relationship ($D = 0.85 \times \mathrm{WS} - 121.21$) between water loss through drainage ($D$) and water supply (WS) irrespective of the cropping system. These authors defined WS as the residual soil water from previous fall (0- to 3-m soil depth) plus the hydrological year precipitation. The above relationship shows that stored soil water is important in accounting for annual drainage losses. For all cropping systems tested in Randall et al. (1997) study, subsurface drainage occurred when water supply was >1426 mm (Huggins et al., 2001). Above this threshold, water loss by drainage was 85% of the water supply.

Similar to water use studies by native grasses, water use studies have also been conducted on present day row crops such as corn and soybean. Using eddy covariance measurements with small towers, Suyker and Verma (2009) showed that growing season (May–September) ET from rainfed corn and soybean in Eastern Nebraska varied between 420 and 505 mm yr$^{-1}$. The corresponding annual values ranged from 553 to 656 mm. At the same site, growing season ET for irrigated corn and soybean ranged from 430 to 586 mm with annual values varying from 566 to 746 mm. Using the Mapping Evapotranspiration at High Resolution with Internalized Calibration (METRIC) model, Khand et al. (2017) estimated the growing season corn ET of 464 and 461 mm in 2009 at drained and undrained sites, respectively, in southeastern North Dakota (bordering Minnesota and South Dakota). These low ET values for corn were due to a very cool summer in North Dakota. Comparatively, the growing season ET of soybean in the same area in 2010 were 514 and 567 mm for the drained and undrained fields, respectively. In southeastern South Dakota (bordering Minnesota and Iowa), growing season ET of corn in tile drained and undrained fields in 2013 were 683 and 684 mm, respectively (Khand, 2014). Based on a literature search, Gupta et al. (2015) concluded that annual water loss for corn and soybean by evapotranspiration ranged from 550 to 650 mm compared with about 350 mm plus non-growing season soil evaporation for small grains, and 581 mm plus non-growing season evaporation for alfalfa.

Considering the recent emphasis on the development of bio-energy crops, several other studies have compared water use by high biomass-producing grasses relative to corn and soybean. For example, Hamilton et al. (2015) showed that perennial grasses (a five-species native grass assemblage or 18 species restored prairie) and annual row crops used approximately the same amount of water when grown under similar conditions in Michigan. The five native grass assemblage were big bluestem (*Andropogon gerardii* Vitm.), Canadian wildrye (*Elymus canadensis* L.), switchgrass (*Panicum virgatum* L.), little bluestem [*Schizachyrium scoparium* (Michx.) Nash], and Indiangrass [*Sorghastrum nutans* (L.) Nash]. Annual ET for three normal precipitation years (2010, 2011, and 2013) ranged from 449 to 629 mm for prairie grasses compared with 462 to 549 mm for corn and soybean. Using the eddy covariance technique, another similar study in Michigan (Abraha et al., 2015) showed that ET from CRP grassland varied from 622 to 706 mm compared with 480 to 639 mm for annual and perennial crops. A recent study by Garcia y Garcia and Strock (2018) at Lamberton, MN, showed that April–October ET for alfalfa, corn, and soybean over 3 yr (2013 to 2015) were 652, 535, and

484 mm, respectively. Comparatively, the average water use by the prairie in this study was 604 mm.

The objective of this research was to estimate ET of corn and soybean relative to those of native grasses using the METRIC model in West Central Minnesota, an area representative of the Minnesota River Basin. This information is gathered to assess to what degree (if any) the replacement of prairies and small grains by corn and soybean would have affected recent streamflows in the Minnesota River Basin.

## METHODS

Several methods are available for measuring ET of various crops. These include water balance, lysimeter, and the eddy covariance technique. However, all these methods are expensive, time consuming, and may not fully capture the spatial heterogeneity within or among fields. With the availability of satellite imagery like that from Landsat, efforts have also been made to estimate ET from the satellite data. Two such methods include the Surface Energy Balance Algorithms for Land (SEBAL) by Bastiaanssen et al. (1998 a, 1998b) and the Mapping Evapotranspiration at High Resolution using Internalized Calibration (METRIC) model of Allen et al. (2007). The METRIC model is an extension of the SEBAL method (Tasumi et al., 2005; Allen et al., 2007). An advantage of satellite-based methods is that they allow for a more precise estimate of energy balance variables over a large area on a pixel-by-pixel basis, thus accounting for variability in plant growth, plant health, water availability, and canopy cover compared with ground-based estimations at a small plot level (Allen et al., 2007, 2011). Both the SEBAL and the METRIC models assume all residual energy, after the removal of sensible and soil heat fluxes from the net radiation flux, is consumed by evapotranspiration. The key difference between the models is that the SEBAL model is calibrated against a large water body to establish the upper end of the ET range, whereas the METRIC model is calibrated against an alfalfa crop. Use of alfalfa as a reference crop helps to make METRIC predictions consistent with the widely used crop coefficient approach for estimating crop water use.

### The METRIC Model

The latent heat flux estimated as the residual of the energy balance at the land surface in the METRIC model is given in Eq. [1].

$$\mathrm{LE} = R_\mathrm{n} - G - H \qquad [1]$$

where LE is the latent heat flux (W m$^{-2}$), $R_\mathrm{n}$ is net radiation flux (W m$^{-2}$), $G$ is soil heat flux (W m$^{-2}$), and $H$ is sensible heat flux (W m$^{-2}$). Energy balance calculations are done for each pixel (30 × 30 m Landsat resolution) in a satellite image. The METRIC model utilizes shortwave and thermal spectral bands information from common image sources such as the Landsat 5 Thematic Mapper, Landsat 7 Enhanced Thematic Mapper plus, or the Landsat 8 Operational Land Imager and Thermal Infrared Sensor.

The net radiation in Eq. [1] is estimated from short and long wave radiations after accounting for surface reflection and Earth's emissivity (Eq. [2]).

$$R_\mathrm{n} = (1 - \alpha)\mathrm{R_s} + (\varepsilon L_\mathrm{in} - L_\mathrm{out}) \qquad [2]$$

where $\alpha$ is surface albedo, $R_\mathrm{s}$ is short-wave radiation (W m$^{-2}$), $\varepsilon$ is land surface emissivity, and $L_\mathrm{in}$ and $L_\mathrm{out}$ are incoming and outgoing long-wave radiation (W m$^{-2}$), respectively. The $R_\mathrm{s}$ value is calculated using the theoretical curve for clear sky radiation and the transmissivity of the atmosphere (Allen, 1996), $\alpha$ is determined by integrating spectral reflectances across the short-wave bands of the Landsat image (Tasumi et al., 2005), and the value of $L_\mathrm{in}$ and $L_\mathrm{out}$ are calculated using surface temperature derived from satellite images (Tasumi et al., 2005).

Soil heat flux, $G$, is empirically determined from leaf area index (LAI) or indirectly from Normalized Difference Vegetation Index (NDVI) using the functions (Eq. [3a] and [3b]) given by Numata et al. (2017). LAI and NDVI were estimated using the relationships in Eq. [4] and [5] given by Allen et al. (2014) and Tasumi et al. (2005).

$$G / R_\mathrm{n} = 0.05 + 0.18\mathrm{e}^{-0.521\mathrm{LAI}}\ (\mathrm{LAI} \geq 0.5) \qquad [3a]$$

$$G / R_\mathrm{n} = 1.80(T_\mathrm{s} - 273.16) / R_\mathrm{n} + 0.084\ (\mathrm{LAI} \leq 0.5) \qquad [3b]$$

$$\mathrm{LAI} = 7.0 \times \mathrm{NDVI_s}^3 \qquad [4]$$

$$\mathrm{NDVI} = \frac{\mathrm{ref}_4 - \mathrm{ref}_3}{\mathrm{ref}_4 + \mathrm{ref}_3} \qquad [5]$$

where $T_\mathrm{s}$ is the surface temperature (K), $\mathrm{NDVI_s}$ is surface NDVI calculated using the surface reflectances, $\mathrm{ref}_3$ and $\mathrm{ref}_4$ are reflectances from bands 3 and 4 of Landsat 5 and 7, and bands 4 and 5 of Landsat 8, respectively.

Sensible heat flux, $H$, is estimated from Eq. [6] using the difference in near-surface to air temperature at 2 m height ($dT$). Near surface temperature in this study corresponds to a height floating 0.1 m above the zero displacement height (Allen et al., 2007, 2014).

$$H = \frac{\rho \times C_\mathrm{p} \times dT}{r_\mathrm{ah}} \qquad [6]$$

where $\rho$ is air density, which is a function of atmospheric pressure (kg m$^{-3}$), $C_\mathrm{p}$ is specific heat of air (1004 J kg$^{-1}$ K$^{-1}$), and $r_\mathrm{ah}$ is aerodynamic resistance to heat transport (s m$^{-1}$) estimated from wind speed and estimates of atmospheric stability. An accurate estimate of the $dT$ is important because it has a large influence on the calculated evapotranspiration values (Choi et al., 2009). Rather than estimating $dT$ directly from surface temperature measurements, $dT$ in the METRIC model is estimated from two extreme conditions in the image referred as "cold" and "hot" pixels (Allen et al., 2007; Numata et al., 2017). These extreme conditions represent the near maximum and minimum surface temperatures within the image. A cold pixel is usually defined as having high vegetative growth (high NDVI > 0.75 and high LAI), and a low surface temperature resulting from evaporative cooling representative of an actively growing and transpiring crop. The hot pixel is defined as having little to no plant cover (low NDVI ~0.2, and low LAI) and a high surface temperature representative of a dry, bare soil surface. A surface soil water balance is used to account for evaporation of residual soil moisture from antecedent rainfall events at the hot pixel. Choosing a set of cold and hot pixels is an iterative process, ensuring that the selected pixels accurately represent the climatic and crop growth conditions within the image for model accuracy. After the final cold and hot anchor pixels have been selected, a linear relationship is established between the $dT$ vs. surface temperature for the cold and hot pixels. The $dT$ values for all other pixels within an image are then estimated from this linear regression function. Further details on the selection of cold and hot pixels are described in Numata et al. (2017).

After estimating $LE$ from Eq. [1], the next step in calculating ET is converting latent heat flux into instantaneous evapotranspiration ($ET_{inst}$) and estimating the fraction of reference ET $(ETrF)_i$ of each pixel.

$$ET_{inst} = 3600 \frac{LE}{\lambda} \quad [7]$$

$$(ETrF)_i = \frac{ET_{inst}}{ET_r} \quad [8]$$

where 3600 refers to seconds in 1 h, $\lambda$ is the latent heat of vaporization, and $i$ refers to the $i$-th pixel number. The variable ETrF is equivalent to the well-known concept of crop coefficient ($K_c$) in the literature (Numata et al., 2017). Reference ET ($ET_r$) is calculated at hourly time steps using the alfalfa-based ASCE standardized Penman–Monteith equation (Eq. [9]) and hourly weather data (ASCE-EWRI, 2005; Tasumi et al., 2005).

$$ET_r = \left[ \frac{0.408\Delta(R_n - G) + \gamma \frac{C_n}{T+273} u_2 (e_s - e_a)}{\Delta + \gamma(1 + c_d u_2)} \right] \quad [9]$$

where $C_n$ and $C_d$ are constants that change with crop reference type (alfalfa, grass), $T$ is the air temperature in degrees Celsius, $u_2$ is the mean daily or hourly wind speed at 2-m height (m s$^{-1}$), $(e_s - e_a)$ is the vapor pressure deficit of the air, $e_s$ is saturation vapor pressure, $e_a$ is actual vapor pressure, $\Delta$ is slope of the saturated vapor pressure curve as a function of air temperature, and $\gamma$ is the psychrometric constant. Instantaneous ETrF $(ETrF)_i$ is assumed to be representative of the daily ETrF (Allen et al., 2007, 2011). Estimates of ETrF on satellite overpass dates are commonly interpolated between image dates to construct crop coefficient curves for each pixel using cubic spline or polynomial functions (Allen et al., 2007; Kjaersgaard et al., 2011).

The actual evapotranspiration ($ET_a$) for each area of interest (AOI) was calculated using an average value of $\overline{(ETrF)_i}$ over all pixels in the AOI and the ETr value (Eq. [10]). Depending on the size of the AOI, the number of pixels can vary.

$$ET_a = \overline{(ETrF)_i} \times ET_r \quad [10]$$

Allen et al. (2007) showed that METRIC-predicted ET on a seasonal basis were within 4% of measured values at Montpelier, ID. Similar tests on sugarbeet (*Beta vulgaris* L.) field at Kimberly, ID, showed less than 1% error in ET measurements (Allen et al., 2007). Choi et al. (2009) stated that when used correctly, the METRIC method can be accurate. However, these authors noted that there can be a bias in predicted ET values if incorrect cold and hot pixels are selected in a given image.

## Site Set-Up and Data Inputs

The METRIC model was used to estimate ET values of irrigated and non-irrigated corn, and non-irrigated soybean from June to October, and of wetlands, and five differently managed prairie areas from May to October during 2015. The study units were located near the town of Appleton in West Central Minnesota (Fig. 1). Corn and soybean fields were located north and west of Appleton, whereas the Chippewa Prairie Reserve and the wetland areas were south of Appleton along a stretch of the Minnesota River. The Chippewa Prairie Reserve and wetlands are under the joint management of the Minnesota Department of Natural Resources (MNDNR) and the Nature Conservancy. This prairie was established in 1971; however, not all sections of the prairie under investigation are that old. Sections of the prairie were previously used for hay and grazing operations. The total prairie area is roughly 13 km$^2$ and are located within Swift and Chippewa counties in Minnesota.

A total of 12 corn fields (6 irrigated and 6 non-irrigated) and 6 non-irrigated soybean fields were identified within the satellite images in the study area for ET calculations. Irrigated corn parcels were identified from circular shapes representing pivot irrigation. Comparatively, non-irrigated corn areas were identified as areas without center pivot circles in the satellite images. Identification of the corn and soybean crops was done using the USDA CropScape map layer for the study year (https://nassgeodata.gmu.edu/CropScape/). Area farmers were also contacted for ground truthing of the CropScape data. CropScape accurately portrayed the crops that the farmers grew. Aerial imagery collected by Pictometry International Corporation for Swift County (http://www.gismidwest.com/maps/swiftpublic/) was used to identify additional irrigation equipment (such as pivots) that might be in the areas of interest but not discernable from the satellite imagery.

The prairie area was split into five sections (Fig. 1) in accordance with the Minnesota Biological Survey's subclasses and burning and grazing regimes (Harris, 2014). The five sections were burned and grazed at different times and were thus in different phases of prairie regrowth. We hypothesized that each prairie growth stage would represent a different ET regime, and thus ET estimates were made for each prairie unit separately. The documentation on the state of the prairie vegetation, burn regime, and grazing regime for 2010 to 2013 were taken from published records (Harris, 2014), whereas the burn data for 2014 and 2015 were obtained through personal communication with Fred Harris, MNDNR plant ecologist and botanist.

During the 2014 growing season, the MNDNR sampled multiple points within the prairie to identify plant species (Harris, 2015). Some of the main taxa identified in the prairie were: European water-plantain (*Alisma* spp.), sedge grass (*Carex* spp.), tall thistle (*Cirsium* spp.), rosette grasses (*Dichanthelium* spp.), snake grass (*Equisetum* spp.), muhly grasses (*Muhlenbergia* spp.), wood sorrels (*Oxalis* spp.), groundcherries (*Physalis* spp.), Rose *(Rosa* spp.), *and* goldenrod (*Solidago* spp.). Harris (2015) also noted that many areas within each prairie unit were bare soils with intermittent standing water and little vegetation. These depressions also contained plant species that were on the MNDNR threatened list. By mid-summer 2015, the standing water had evaporated from these depressions.

Each year, grazing of varying intensities occurred in all prairie units. The most recently burned prairie unit (Unit 2) had the

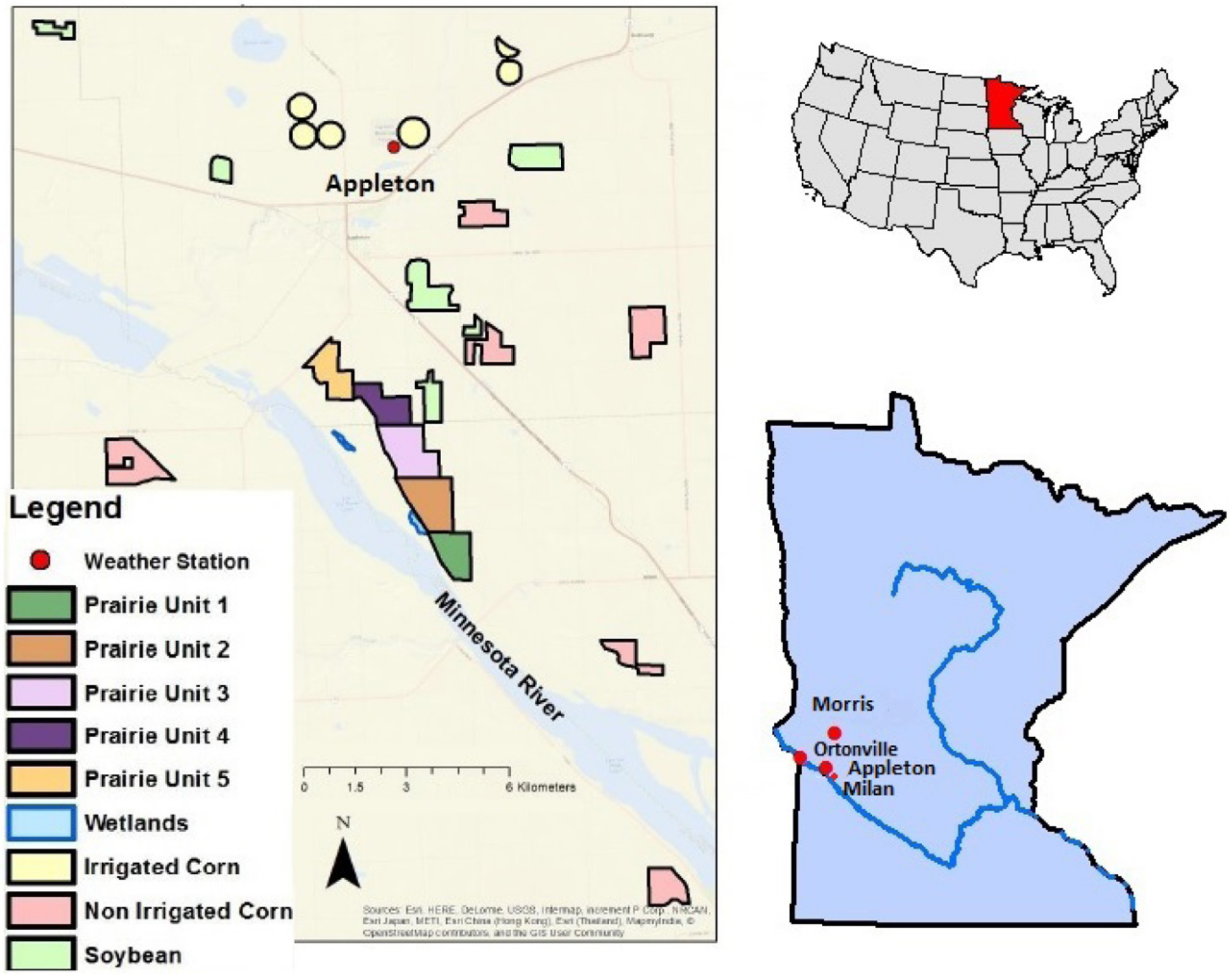


Fig. 1. Chippewa prairie units, corn and soybean fields, the wetlands, and the weather station in the study area near Appleton, MN. Daily solar radiation and 19–30 July 2015 air temperatures for the study area were taken from weather stations at Morris and Ortonville, MN, respectively (shown in the Minnesota map).

highest grazing intensity while the prairie unit with lowest grazing intensity (Unit 1) had been without burning for the longest time. The grazing practice used at the prairie site is called patch-burn grazing, and is a technique that helps establish and control vegetation throughout prairie systems (Harris, 2015). Prairie Unit 1 was burned and most intensively grazed in 2010. Prairie Unit 2 was burned and most intensively grazed in 2015. Prairie Unit 3 was burned and most intensively grazed in 2014. Prairie Unit 4 was burned and most intensively grazed in 2013. Prairie Unit 5 was burned and most intensively grazed in 2012.

A total of nine images covering the 2015 growing season (May–October) were downloaded from the USGS GloVis website and used for the METRIC ET analysis. These images were taken from both Landsat 7 and Landsat 8 (Supplemental Table S1). Images were selected for days with no cloud cover over the field and prairie AOI parcels.

All images and maps were projected to the WGS 84, UTM 14N coordinate system. The ET calculations from the METRIC program were done on a full Landsat scene approximately 185 by 170 km in size. Since each AOI had a different areal coverage, average monthly ET was calculated as the average monthly ET from all pixels except for a 30-meter buffer inward from field edges in each AOI. The 30 m buffer along the field edges was left out of calculations to reduce impacts from mixed pixels. Monthly ET values were then further averaged across the corn, soybean, and wetland areas, depending on the number of AOI of a given land cover type. For each crop species and wetland area, the monthly values from 1 May to 22 October for prairie and wetlands and 8 June to 22 October for corn and soybean were then summed together to estimate growing season ET. Since no vegetation is growing in late fall and soils are frozen during winter, no ET calculations were made from before 1 May or after 23 October.

In the event that a cold or hot pixel selected during the first round of pixel selection did not represent the extreme ends of the ET for a given satellite overpass, an alternate pixel was selected and the calculations repeated. For some satellite overpass dates, over 10 iterations were performed to find representative hot and cold anchor pixels.

The internal calibration portion of the METRIC model requires detailed weather information including wind speed for calculating $ET_r$. The nearest weather station to the Chippewa native prairie was located 8 km to the northeast at the Appleton Municipal Airport (AQP) (Fig. 1). There were no obstructions that would affect the wind speed measurements and the placement of the runway likely had none to negligible impact on air temperature measurements. Therefore, the data at this site were deemed acceptable for calculating the reference ET

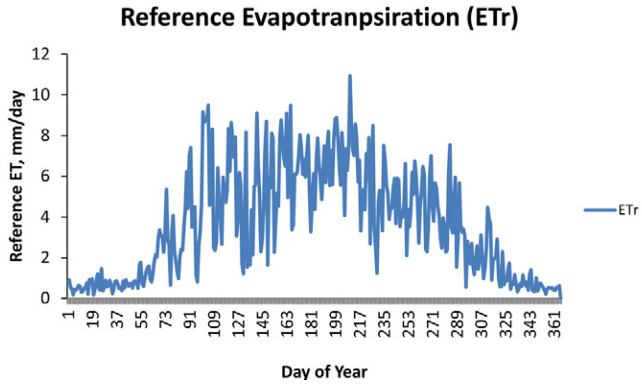


Fig. 2. Daily variation in evapotranspiration of alfalfa (reference crop, ETr) in 2015 as calculated using the Penman–Monteith Standardized Equation.

(ASCE-EWRI, 2005). The weather data at AQP were downloaded from the Iowa Environmental Mesonet (IEM) using the airport identifier (https://mesonet.agron.iastate.edu/). The weather data included precipitation, air, and dew point temperatures and wind speed. The wind speed was measured at 10 m above the ground surface and was adjusted to wind speed at 2 m using the logarithmic wind profile equation (ASCE-EWRI, 2005). The daily minimum, maximum and the average of the hourly values for air temperature, wind speed, precipitation, and dew point were then used to calculate ETr.

Since air temperature data for the Appleton Municipal Airport was not available from 19 to 30 July 2015, these data were taken from the Ortonville (Minnesota map in Fig. 1) weather station, which lies about 37 km northwest of the AQP weather station. To ensure Ortonville temperatures were consistent with AQP temperatures, a regression relationship was developed between the temperatures for the two sites covering the period 1 to 18 July. The linear relationship ($y = 1.04x - 0.03$; $R^2 = 0.95$; where $y$ is air temperature at AQP and $x$ is air temperature at Ortonville) was then used to adjust Ortonville air temperatures to get an estimated temperature at the Appleton Municipal Airport for 19 to 30 July 2015.

Solar radiation data was taken from the University of Minnesota at Morris, MN (Eric Buchanan, personal communication, 2016). The above weather station is about 56 km north of the prairie (Minnesota map in Fig. 1) and is the closest station that had daily solar radiation measurements for 2015. Although solar radiation can exhibit daytime variability due to passing clouds and weather systems, it generally exhibits more homogeneity on seasonal and annual scales and is broadly representative of the surrounding area (K. Blumenfeld, personal communication, 2018).

A comprehensive weather data quality control process was completed for all the weather data described above using Allen (1996) and ASCE-EWRI (2005). The weather data was used for two applications. First, these data were used to calculate hourly ETr. The second application of the wind speed was for calibration of parameters within the METRIC program for each satellite overpass date.

Since there was a failure of the on-board scan line corrector of Landsat 7 in 2003, there were wedge-shaped data gaps extending inward from the image edges for all images captured after 2003 (https://landsat.usgs.gov/landsat-7). To correct for these data gaps, a gap filling calculation to fill in missing ETrF

Table 1. Total precipitation and average monthly temperature at Appleton Municipal Airport for 5 mo in 2015, over which ET calculations were made using the METRIC model.

| | Month | | | | |
|---|---|---|---|---|---|
| Variable | May | June | July | August | September |
| Precipitation, mm | 188 | 50 | 40 | 111 | 11 |
| Temperature, °C | 14.3 | 20.9 | 23.2 | 20.5 | 19.6 |

estimates was performed that calibrated the gapped areas with the surrounding area assuming a data gradient over the gapped areas (Allen et al., 2014). Landsat 8 images had no data gaps and no corrective action was needed to fill data gaps.

An output from the METRIC model are 24-h ETrF values for each pixel. These 24-h ETrF values within each AOI were first averaged and then multiplied with the ETr value to calculate ETa for each AOI. Since there were only nine satellite images, ETrF values between the satellite image dates were extrapolated using a cubic spline function or a second-degree polynomial. The ETa values reported in this article are averages for various vegetation type and wetlands. Irrigated corn, non-irrigated corn, and irrigated soybean ETa are averages over six measurements each, whereas previously burned prairie and wetland ETa are averages over four and two measurements, respectively. There was only one ETa measurement for recently burned prairie.

## RESULTS

### Reference Evapotranspiration, ETr

Figure 2 shows the distribution of daily ETr in 2015. The ETr values in 2015 ranged from 0 to 11 mm $d^{-1}$. Table 1 summarizes the monthly weather data in 2015 at the Appleton airport. Mean annual air temperature in 2015 at Appleton was 8.7°C. Although long-term air temperatures are not available for the Appleton airport, a comparison with 2015 mean annual air temperature (9.2°C) and 30-yr normal (1981–2010) air temperature (7.5°C) at Milan, MN (13 km SW of Appleton) suggest that 2015 at Appleton was warmer than average. Appleton precipitation for 2015 was 599 mm. Comparatively, Milan precipitation for 2015 was 634 mm, 30 mm below normal. There were three large rain events at Appleton during the 2015 growing season—55 and 81 mm in May, and a 90-mm rain event spanning 2 d in August.

### Fraction of Reference ET, ETrF

Figures 3 to 5 show temporal distribution of ETrF values among prairie, wetlands, and crops in the study area. Depending on the size of AOI, the number of pixels varied from 124 to 1495 (Supplemental Table S2). For the prairie and wetland AOIs, there was a small dip in ETrF values around DOY 215. The reason for the dip in ETrF values is not apparent but follows several weeks of limited rainfall. One hypothesis for the dip is that around DOY 170 there was a larger rainfall event that likely brought the soil moisture content up to near field capacity, resulting in relatively high ET from the "previously burned" sections that had well established grass ready to transpire. However, in the recently burned prairie system, plants were just establishing themselves, so the ET rates were lower until around DOY 195 when the grass was fully reestablished after the burn.

The smaller rainfall events that occurred around DOY 190 and 200 were not large enough to increase the soil moisture and was likely lost quickly to evapotranspiration. The same was the case around DOY 225, yet the ETrF curve was on the upswing. The reason for this upswing may be that a satellite overpass occurred on DOY 223, which caught some of this immediate "burn off" of moisture from the small rain event resulting in higher ETrF values. Finally, around DOY 230 a larger rain event helped to refill the soil profile thus causing the ET values to rise again. The following text discusses the differences in ETrF distribution by land use.

## Prairie Units

The ETrF values for Prairie Units 1, 3, 4, and 5 were similar until around DOY 200 and then there was some divergence in their distributions (Fig. 3). Comparatively, ETrF values of Prairie Unit 2 were always lower than the other prairie units and also had a more prominent dip on DOY 170 and 215. We hypothesized that lower ETrF values for Prairie Unit 2 relative to other prairie units was likely due to a burn that took place in the spring of 2015. The idea that the spring burn could be the cause of lower ETrF values was further investigated by looking at the NDVI of Prairie Unit 2 vs. other prairie units. It was found that Prairie Unit 2 always had 0 to 25% lower NDVI compared with the other prairie units. The largest difference in NDVI between Prairie Unit 2 and other prairie units took place in May and June; the months when the prairie was burned. Furthermore, Prairie Unit 2 was intensively grazed after the burn for rest of the year. Thus, it is likely that the dip was due to stunted prairie growth, resulting in reduced ET. Although ETrF values of Prairie Units 1, 3, 4, and 5 were slightly different from each other after DOY 200, the overall difference in ET values was similar for the year (discussed later). Considering these small differences, the ETrF values of Prairie Units 1, 3, 4, and 5 were averaged and designated as "previously burned" prairies (Fig. 4). Comparatively, ETrF values of Prairie Unit 2 reflected a "recently burned" prairie. Unit 2 represents a special case in the application of METRIC. Considering the presence of black ash at the soil surface and the vegetation growth being somewhat stunted due to recent burn, METRIC may have tended to overestimate ETa in Unit 2. In other words, the vegetation was sparse enough for the black ash to reduce albedo while at the same time dense enough for the Landsat thermal band to sense the surface temperature relatively cool. The result would have been an increase in energy at the soil surface, which METRIC may have translated into a slight overestimation of ETa.

## Wetlands

The distribution of ETrF values for the wetland relative to previously burned and recently burned prairie units are shown in Fig. 4. ETrF for wetlands started high and stayed higher for most of the growing season. Similar to other units, there was a slight dip in ETrF values in mid-August (DOY 215). This dip in wetland ETrF values is hypothesized to be from a reduced water level in wetlands from prolonged period without precipitation.

## Row Crops

The distribution of daily ETrF values for corn and soybean are shown in Fig. 5. ETrF values of row crops were fitted with a second-degree polynomial rather than a cubic spline function used in fitting the ETrF values from the prairies and the wetlands units. This departure in curve fitting technique was adopted

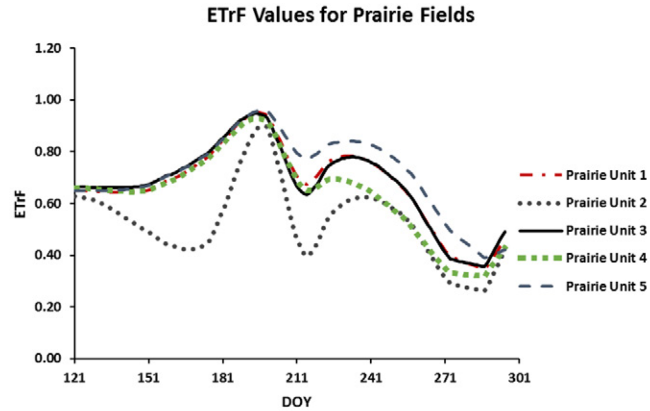


Fig. 3. Temporal variation in daily ET as a fraction of ET from a reference crop (ETrF) for various prairie units at the Chippewa Prairie Reserve during the 2015 growing season. ETrF values in this graph are fitted values using a cubic spline function.

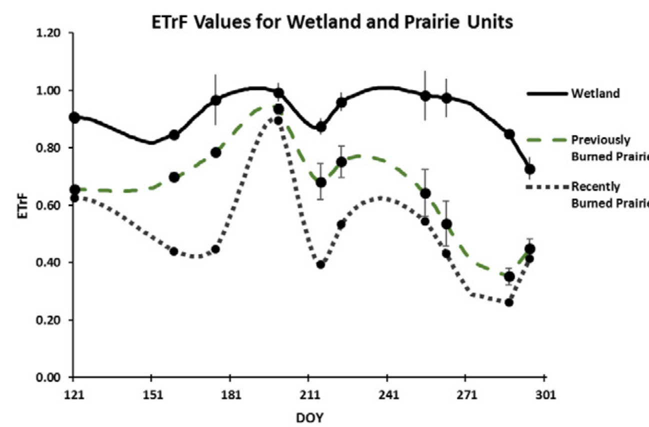


Fig. 4. Temporal variations in ET as a fraction of ET from a reference crop (ETrF) for wetlands, previously burned prairies, and recently burned prairie at the Chippewa Prairie Reserve during the 2015 growing season. ETrF values in this graph are fitted values from a cubic spline function. Vertical bars are standard deviations around the mean.

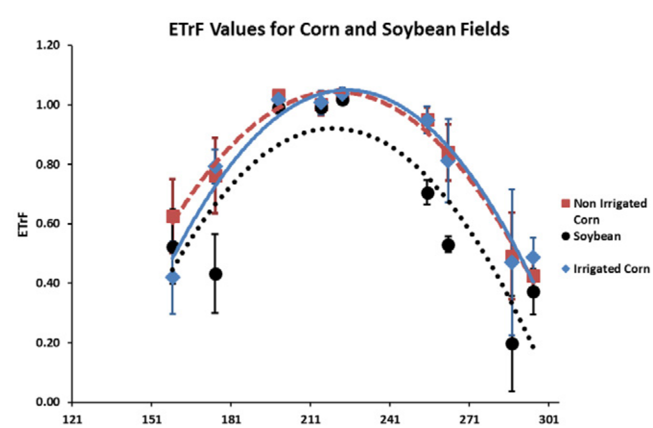


Fig. 5. Temporal variation in ET as a fraction of ET from a reference crop (ETrF) for irrigated-corn, non-irrigated corn and non-irrigated soybean fields at Appleton, MN during the 2015 growing season. Each point is an average of six AOI units of similar crop type. Vertical bars are standard deviation around the mean. ETrF values in this graph are fitted values from a second-degree polynomial.

Table 2. A second-degree polynomial fit of ETrF for irrigated and non-irrigated corn and non-irrigated soybean. *Y* is the ETrF values and *X* is day of the year (DOY).

| Crop type | Best fit second degree polynomial | $R^2$ |
|---|---|---|
| Irrigated corn | $Y = -1.31E-04X^2 + 0.059X - 5.55$ | 0.95 |
| Non-irrigated corn | $Y = -1.16E-04X^2 + 0.051X - 4.59$ | 0.98 |
| Soybean | $Y = -1.30E-04X^2 + 0.057X - 5.32$ | 0.77 |

because of a problem fitting the spline function as well as to more accurately represent the evapotranspiration of the row crops. For example, the ETrF values of corn and soybean for 29 April image were high (0.75 and 0.66, respectively; likely due to high evaporation from a bare black soil on a sunny day from the black soil). This is based on the observations that the row crops were planted on 15 April in the area and the temperatures were less than normal after planting. Thus, it was unlikely that most emergence had occurred by 29 April and there was a substantial crop ET. In addition, the METRIC estimated ETrF values for corn and soybean from the 8 June image were less than those on 29 April (0.42 and 0.52, respectively). A combination of these high and low ETrF values early in the season caused the cubic spline function routine to "over-fit" when fitting ETrF values from 29 April to 22 October. A similar "over-fitting" of the cubic spline function routine occurred again when fitting ETrF values from 8 June to 30 September. To overcome these problems with the cubic spline function subroutine and since the truncated data from 8 June to 22 October (DOY 159–295) showed a bell shaped distribution (Fig. 5), we decided to fit a second-degree polynomial to ETrF values of row crops. Table 2 lists the second-degree polynomial equations for temporal variation of ETrF in row crop fields.

Considering there was substantial variability within an AOI, we calculated one ETrF value for each AOI by averaging the ETrF over all pixels. These averaged ETrF values were further averaged by land cover type to create one ETrF value for each land cover in our study. Figure 5 shows the distribution of averaged ETrF for irrigated and non-irrigated corn and non-irrigated soybean.

A comparison of ETrF values of corn and soybean with native grasses (Fig. 6) showed that ETrF values behaved similarly for all vegetation types for about 40 to 50 d at the start of the season. However, the ETrF value for native grasses peaked around DOY 200 followed by a steep decline. Around DOY 215, the ETrF value of native grasses recovered somewhat before flattening out and then decreased again. The recently burned prairie units followed a similar cycle as the previously burned prairie, but the peak was not as high. Furthermore, the recovery of ETrF values was much lower after DOY 215 (Fig. 6). The maximum ETrF values of native grasses was slightly lower than those of corn and soybean (Fig. 6). Also, the ETrF values of non-irrigated corn were slightly higher than those of irrigated corn in both initial and final periods (Fig. 6). However, there was not much difference between the irrigated and non-irrigated corn ETrF values near the peak of the growing season.

## Evapotranspiration

Evapotranspiration (ETa) of a given vegetation type and wetland was calculated by multiplying the averaged 24-h ETrF value in Fig. 3 to 5 for a given vegetation with the 24-h ETr value in Fig. 2. A summary of monthly and growing season ETa values for various vegetation type and wetland in the study

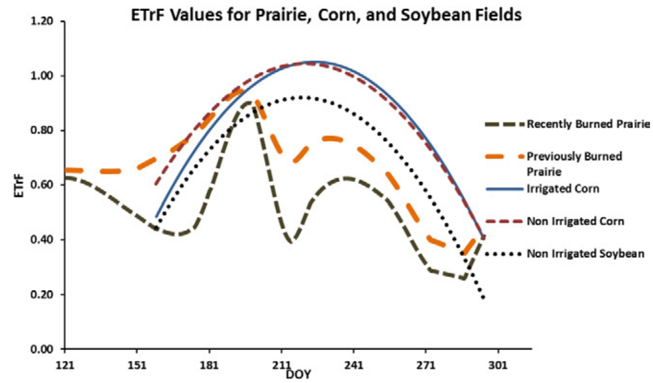


Fig. 6. A comparison of ETrF values among various vegetation type (irrigated corn, non-irrigated corn, non-irrigated soybean, recently burned prairie, and previously burned prairie) during the 2015 growing season. These curves are the best curves in Fig. 4 and 5.

area are listed in Table 3. Among the studied landscape units, the ETa values from 8 June through 22 October followed the trend: wetland (717 mm) > rain fed corn (662 mm) > irrigated corn (647 mm) > rain fed soybean (554 mm) > previously burned prairie (537 mm) > recently burned prairie (406 mm). Comparatively from 1 May to 22 October, the ETa of wetland, previously burned and recently burned prairie grasses were 884, 665, and 513 mm, respectively. Considering the variability in ETrF values in Fig. 6 the differences in seasonal ETa values among the various vegetation types (except for recently burned prairie) are not likely large. However, there were some differences in temporal ETa distribution between the vegetation types. For example, ETa values for the prairie units were generally higher in early spring whereas they were higher during mid-summer for corn and soybean. This is expected considering native prairies in the area are mostly $C_3$ type plants (efficient in photosynthesis in cool and wet season) with a greening up earlier in the spring compared to corn which are $C_4$ type of plants with more photosynthesis and thus more ET in hot summer weather.

The above findings of small differences in ET among various vegetation types suggest that it is unlikely that the changeover from prairie systems to row crop agriculture in the Minnesota River Basin had a large impact on landscape evapotranspiration. A comparison of June–October irrigated and non-irrigated corn (647–662 mm) and non-irrigated soybean (554 mm) ET relative to prairie ET (406–537 mm) would suggest that the landscape evapotranspiration has likely increased with the introduction of row crop agriculture. However, a comparison of longer season (May–October) prairie ET (513–665 mm) to June–October corn and soybean ET (647–662, 554 mm) would suggest small differences in ET between the native prairies and the row crop agriculture. The native prairie ET also showed a wide variation among the prairie units in the study area depending on how the prairie units were managed. For example, there was a decrease in ET when the prairies were burned and grazed. These differences in prairie management further points out that a reduction in ET may occur if the native prairies were reintroduced in the landscape to replace row crop agriculture and occasionally burned and grazed.

## DISCUSSION

Overall, the METRIC calculated ETa values for wetlands were within the range of values found in the literature. ETa of

Table 3. The METRIC estimated monthly evapotranspiration (ETa) for various land uses (vegetation types and wetlands) near Appleton, MN, in 2015. ETa of corn and soybean are averages over six observations whereas ETa of previously burned prairies and wetlands are averages over four and two observations, respectively.

| | | Prairie | | Corn | | Soybean | Wetlands |
|---|---|---|---|---|---|---|---|
| Month | ETr | Previously burned | Recently burned | Irrigated | Non-irrigated | Non-irrigated | Wetland |
| | ET, mm | | | | | | |
| May | 155 | 101 | 88 | – | – | – | 134 |
| June | 190 | 141 | 86 | 97 | 111 | 89 | 172 |
| July | 214 | 185 | 155 | 202 | 208 | 181 | 206 |
| Aug. | 166 | 123 | 89 | 172 | 171 | 150 | 159 |
| Sept. | 142 | 83 | 67 | 126 | 123 | 101 | 139 |
| Oct.† | 87 | 33 | 26 | 50 | 49 | 32 | 74 |
| Sum‡ | 798 | 537 | 406 | 647 | 662 | 554 | 717 |
| Seasonal sum§ | 954 | 666 | 511 | – | – | – | 884 |

† October sum is from 1–22 Oct.

‡ Sum represents the period 8 June–22 Oct.

§ Seasonal sum represents the period 1 May–22 Oct.

the other vegetation types (Table 3) were on the upper end of the calculated and observed values reported in the literature. For example, Shjeflo (1968) reported that the growing season evaporative losses for 10 potholes and wetlands in North Dakota varied from 134 to 796 mm in 1960–1964. During that period, there were some potholes that went dry and there was no evaporative loss. For four Minnesota lakes, the measured evaporative losses in 1967 varied from 554 to 672 mm (Allred and Manson, 1971). Bauder and Ennen (1981) reported average growing season (1977, 1978) corn and soybean water use for four locations in North Dakota and northwestern Minnesota at 422 and 431 mm, respectively. Comparatively, average growing season water use for spring wheat (*Triticum aestivum* L.), barley (*Hordeum vulgare* L.), and flax (*Linum ussitisimum* L.) were 303, 321, and 349 mm, respectively. Based on water balance over 5 yr (1989–1993), Huggins et al. (2001) reported ET of 531, 523, 531, 591, and 552 mm for continuous corn, corn in corn–soybean rotations, soybean in soybean-corn rotations, alfalfa and grasses associated with CRP, respectively. McKenzie and Woods (2011) summarized the crop water requirements for Alberta, Canada at 540 to 680 mm for alfalfa, 580 to 650 mm for corn silage, 500 to 550 mm for timothy (*Phleum pratense* L.) hay, 420 to 480 mm for spring wheat, 400 to 430 mm for winter wheat, 340 to 440 mm for flax, and 380 to 430 mm for barley. Based on the historical yield of native hay and crop water use vs. yield of alfalfa, Gupta et al. (2015) estimated ET of native hay at 242 mm. Comparatively, the historical ET of alfalfa using the yield vs. water use relationship corresponded to 581 mm (Gupta et al., 2015). Based on Penman–Monteith and water balance equations, Garcia y Garcia and Strock (2018) showed that water use of native prairie in southwestern Minnesota was only slightly higher than those of corn and soybean. The average ET from 2013–2015 in their study followed the trends: alfalfa (652 mm) > prairie (604 mm) > corn (535 mm) > soybean (484 mm). The corresponding ET for the oat–alfalfa mixture was 340 mm. The 2015 ETa values estimated for prairie, corn and soybean using the METRIC model are within the range of ET values reported by Garcia y Garcia and Strock (2018) for 2015 at Lamberton, MN; 142 km south from Appleton. The METRIC model calculated ETa values are also within the range of values reported by Huggins et al. (2001) for corn, soybean, and CRP land at Lamberton, MN. Both these data points from the literature give some confidence that the METRIC estimated ET values for corn, soybean, and prairies in southwestern Minnesota are reasonable. The presence of only small differences in METRIC estimated ET values between row crop and prairies is similar to the findings of Abraha et al. (2015), who concluded that crop water use between row crops and prairies is not likely going to be different because of large variability in precipitation and the soil water availability. The higher value of ET for native prairies in this study compared to earlier studies in North Dakota (Smika et al., 1965; Power, 1985) would suggest that ET of prairie grasses may not only be linked to type of plant species but also to soil water availability. In other words, higher ETa in the prairie units in our study is likely due to higher precipitation in our region compared with North Dakota in earlier studies. However, further studies will be needed to sort out the effects of species and soil water availability on ET of native prairies.

The ET values from this research provide another data point in the discussion relating climate and land cover change impacts on streamflows. As discussed in the introduction, the reason behind why streamflow has been increasing is still intensely debated. The results from the METRIC model indicate that ET losses from prairie and row crop agriculture are somewhat similar on an annual basis. Furthermore, corn and soybean replaced not only the prairies but also oat and other small grains, which has lower ET than that of corn and soybean. Thus, the above analysis shows that it is unlikely that replacement of prairies and small grains by corn and soybean starting in 1940s drastically changed landscape ET in the Minnesota River Basin. Considering that the annual ET is similar but annual precipitation has increased from 50 to 100 mm in the Upper Midwest (Melillo, 2014; Gupta et al., 2015) would suggest that the increased streamflows in recent years are mainly driven by increased precipitation. This is consistent with the findings of Gupta et al. (2015, 2018), who showed that recent higher streamflows are not only due to excess precipitation in the current year but also due to soil-stored water from previous years above average precipitation.

## CONCLUSIONS

Relative estimates of ET from corn and soybean versus prairie grasses are needed to address the question if recent increases in streamflow are primarily from increased precipitation or decreased ET from conversion of small grains and prairie grass ecosystem to current row crop agriculture starting in 1940s.

The study determined ET of wetlands, corn, soybean, and native prairie grasses using the METRIC model. For a period from 8 June through 22 Oct. 2015, the ETa followed the trend: wetland (717 mm) > non-irrigated corn (662 mm) > irrigated corn (647 mm) > non-irrigated soybean (554 mm) > previously burned prairie (537 mm) > recently burned prairie (406 mm). Comparatively from 1 May to 22 October, the ETa of wetland, previously burned and recently burned prairie grasses were 884, 666, and 511 mm, respectively. As expected, there was some seasonal variability in the ET values between different units; higher ET of native prairie grasses in early spring compared with higher ET in mid-summer for row crops. Considering low ET small grains were also part of the landscape previous to the adoption of soybean in the Upper Midwestern United States, we conclude that annual landscape ET has not changed much as a result of soybean adoption replacing prairie and small grains. Considering that annual precipitation has increased from 50 to 100 mm in recent years in the Upper Midwest, this further supports our earlier conclusion that increased streamflows in recent years are primarily due to increased precipitation and not due to land cover changes.

## SUPPLEMENTAL MATERIAL

Supplemental material contains (i) dates and path/row locations of images from Landsat 7 and 8 and (ii) pixel count and average area representing various treatments in the study area.

## REFERENCES


Abraha, M., J. Chen, H. Chu, T. Zenone, R. John, Y.J. Su, S.K. Hamilton, and G.P. Robertson. 2015. Evapotranspiration of annual and perennial biofuel crops in a variable climate. Glob. Change Biol. Bioenergy 7:1344–1356. doi:10.1111/gcbb.12239

Allen, R., A. Irmak, R. Trezza, J.M. Hendrickx, W. Bastiaanssen, and J. Kjaersgaard. 2011. Satellite-based ET estimation in agriculture using SEBAL and METRIC. Hydrol. Processes 25:4011–4027. doi:10.1002/hyp.8408

Allen, R., M. Tasumi, and R. Trezza. 2007. Satellite-based energy balance for mapping evapotranspiration with internalized calibration (METRIC)—Model. Model. J. Irrig. Drain. Eng. 133:380–394. doi:10.1061/(ASCE)0733-9437(2007)133:4(380)

Allen, R., R. Trezza, M. Tasumi, and J. Kjaersgaard. 2014. Mapping evapotranspiration at high resolution using Internalized Calibration Application Manual for Landsat Satellite Imagery. Univ. of Idaho, Kimberly, ID.

Allen, R.G. 1996. Assessing integrity of weather data for use in reference evapotranspiration estimation. J. Irrig. Drain. Eng. 122:97–106. doi:10.1061/(ASCE)0733-9437(1996)122:2(97)

Allred, E.R., and P.W. Manson. 1971. Continuation of studies on the hydrology of ponds and small lakes. Tech. Bull. 274. Agric. Exp. Stn., Univ. Minnesota, Minneapolis.

ASCE-EWRI. 2005. The ASCE standardized reference evapotranspiration equation. In: R.G. Allen, I.A. Walter, R.L. Elliot, et al., editors, Environmental and Water Resources Institute (EWRI) of the American Society of Civil Engineers. ASCE-EWRI Standardization of Reference Evapotranspiration Task Comm. Report. ASCE, Reston, VA.

Bastiaanssen, W.G., M. Menenti, R.A. Feddes, and A.A.M. Holtslag. 1998a. A remote sensing surface energy balance algorithm for land (SEBAL). 1. Formulation. J. Hydrol. 212–213:198–212. doi:10.1016/S0022-1694(98)00253-4

Bastiaanssen, W.G., H. Pelgrum, J. Wang, Y. Ma, J.F. Moreno, G.J. Roerink, and T. Van der Wal. 1998b. A remote sensing surface energy balance algorithm for land (SEBAL). 2. Validation. J. Hydrol. 212–213:213–229. doi:10.1016/S0022-1694(98)00254-6

Bauder, J.W., and M.J. Ennen. 1981. Water use of field crops in eastern North Dakota. North Dakota Farm Res. 38:3–5.

Choi, M., W.P. Kustas, M.C. Anderson, R. Allen, F. Li, and J. Kjaersgaard. 2009. An intercomparison of three remote sensing-based surface energy balance algorithms over a corn and soybean production region (Iowa, US) during SMACEX. Agric. For. Meteorol. 149:2082–2097. doi:10.1016/j.agrformet.2009.07.002

Garcia y Garcia, A., and J. Strock. 2018. Soil water content and crop water use in contrasting cropping systems. Trans. ASABE 61:75–86. doi:10.13031/trans.12118

Gupta, S.C., N.W. Baeumler, A.C. Kessler, M.K. Brown, W.M. Schuh, and K.A. Wolf. 2018. Increased precipitation as the main driver of increased streamflow in tile drained watersheds of the Upper Midwestern U.S. Trans. ASABE 61:207–222. doi:10.13031/trans.12279

Gupta, S.C., A.C. Kessler, M.K. Brown, and F. Zvomuya. 2015. Climate and agricultural land use change impacts on streamflow in the Upper Midwestern United States. Water Resour. Res. 51:5301–5317. doi:10.1002/2015WR017323

Hamilton, S.K., M.Z. Hussain, A.K. Bhardwaj, B. Basso, and G.P. Robertson. 2015. Comparative water use by maize, perennial crops, restored prairie, and poplar trees in the US Midwest. Environ. Res. Lett. 10:064015. doi:10.1088/1748-9326/10/6/064015

Harris, F. 2014. Plant community monitoring at the Lac Qui Parle WMA/ Chippewa Prairie Patch-Burn-Graze Project. Progress Report to Minnesota Dep. of Natural Resources and the Nature Conservancy. Minnesota DNR, St. Paul. p. 1–27. http://files.dnr.state.mn.us/eco/mcbs/chippewa_prairie_pbg_veg_monitoring_14jan2014 (accessed 27 Nov. 2018).

Harris, F. 2015. Wetland Basin Survey and plant community monitoring at the Chippewa Prairie Patch-Burn Grazing Project. Preliminary Progress Report to The Nature Conservation for the 2014 Field Season. Minnesota DNR, St. Paul.

Hoogestraat, G.K., and J.F. Stamm. 2015. Climate and streamflow characteristics for selected streamgauges in eastern South Dakota, water years 1945–2013. USGS, Scientific Investigations Rep. 2015–5146. http://pubs.usgs.gov/sir/2015/5146/sir20155146.pdf (accessed 9 Aug. 2018)

Huggins, D.R., G.W. Randall, and M.P. Russelle. 2001. Subsurface drain losses of water and nitrate following conversion of perennials to row crops. Agron. J. 93:477–486. doi:10.2134/agronj2001.933477x

Karl, T.R., and R.W. Knight. 1998. Secular trends of precipitation amount, frequency, and intensify in the United States. Bull. Am. Meteorol. Soc. 79:231–241. doi:10.1175/1520-0477(1998)079<0231:STOPAF>2.0.CO;2

Khand, K. 2014. Estimating impacts of subsurface drainage on evapotranspiration using remote sensing. MS thesis. South Dakota State Univ., Brookings, SD.

Khand, K., J. Kjaersgaard, C. Hay, and X. Jia. 2017. Estimating impacts of agricultural subsurface drainage on evapotranspiration using the Landsat Imagery-Based METRIC Model. Hydrol. Process. 4:49–65. doi:10.3390/hydrology4040049

Kjaersgaard, J., R. Allen, and A. Irmak. 2011. Improved methods for estimating monthly and growing season ET using METRIC applied to moderate resolution satellite imagery. Hydrol. Process. 25:4028–4036. doi:10.1002/hyp.8394

Lins, H.F., and J.R. Slack. 1999. Streamflow trends in the United States. Geophys. Res. Lett. 26:227–230. doi:10.1029/1998GL900291

McKenzie, R.H., and S.A. Woods. 2011. Crop water use requirements. Agdex 100/561-1. Agri-Facts. Alberta Agriculture and Rural Development, Edmonton, Canada. https://open.alberta.ca/dataset/9a017865-5692-464d-92ac-93b5d50558db/resource/c0d20e0c-9f14-4f6d-8144-b8a6bc3452ba/download/5485851-2011-agri-facts-crop-water-use-requirements-revised-100-561-1-2011-11.pdf (accessed 11 Dec. 2018).

Melillo, J.M. 2014. Climate change impacts in the United States: The third national climate assessment. US Gov. Print. Office, Washington, DC. https://www.globalchange.gov/browse/reports/climate-change-impacts-united-states-third-national-climate-assessment-0 (accessed 9 Aug. 2018).

Novotny, E.V., and H.G. Stefan. 2007. Stream flow in Minnesota: Indicator of climate change. J. Hydrol. 334:319–333. doi:10.1016/j.jhydrol.2006.10.011

Numata, I., K. Khand, J. Kjaersgaard, M.A. Cochrane, and S.S. Silva. 2017. Evaluation of Landsat-Based METRIC Modeling to Provide High-Spatial Resolution Evapotranspiration Estimates for Amazonian Forests. Remote Sens. 9:46. doi:10.3390/rs9010046

Power, J.F. 1985. Nitrogen- and water-use efficiency of several cool-season grasses receiving ammonium nitrate for 9 years. Agron J. 77:189–192. doi:10.2134/agronj1985.00021962007700020004x

Randall, G.W., D.R. Huggins, M.P. Russelle, D.J. Fuchs, W.W. Nelson, and J.L. Anderson. 1997. Nitrate losses through subsurface tile drainage in Conservation Reserve Program, alfalfa, and row crop systems. J. Environ. Qual. 26:1240–1247. doi:10.2134/jeq1997.00472425002600050007x

Schilling, K.E., K.-S. Chand, H. Liu, and Y.-K. Zhang. 2010. Quantifying the effect of land use change on increasing discharge in the Upper Mississippi River. J. Hydrol. 387:343–345. doi:10.1016/j.jhydrol.2010.04.019

Shjeflo, J.B. 1968. Evapotranspiration and the water budget of Prairie Potholes in North Dakota. Geol. Surv. Prof. Pap. 585-B. U.S. Gov. Print. Off., Washington, DC.

Smika, D.E., H.J. Haas, and J.F. Power. 1965. Effects of moisture and nitrogen fertilizer on growth and water use by native grass. Agron. J. 57:483–486. doi:10.2134/agronj1965.00021962005700050024x

Smika, D.E., H.J. Haas, G.A. Rogler, and R.J. Lorenz. 1961. Chemical properties and moisture extraction in rangeland soils as influenced by nitrogen fertilization. J. Range Manage. 14:213–216. doi:10.2307/3895152

Suyker, A.E., and S.B. Verma. 2009. Evapotranspiration of irrigated and rainfed maize–soybean cropping systems. Agric. For. Meteorol. 149:443–452. doi:10.1016/j.agrformet.2008.09.010

Tasumi, M., R.G. Allen, R. Trezza, and J.L. Wright. 2005. Satellite-based energy balance to assess within-population variance of crop coefficient curves. J. Irrig. Drain. Eng. 131:94–109. doi:10.1061/(ASCE)0733-9437(2005)131:1(94)

Wang, D., and M. Hejazi. 2011. Quantifying the relative contribution of the climate and direct human impacts on mean annual streamflow in the contiguous United States. Water Resour. Res. 47:W00J12. doi:10.1029/2010WR010283

Weaver, J.E., and J.W. Crist. 1924. Direct measurement of water loss from vegetation without disturbing the normal structure of the soil. Ecology 5:153–170. doi:10.2307/1929013

Weaver, R.J. 1941. Water usage by certain native grasses in prairie and pasture. Ecology 22:175–192. doi:10.2307/1932213

Xu, X., B.R. Scanlon, K. Schilling, and A. Sun. 2013. Relative importance of climate and land surface changes on hydrologic changes in the US Midwest since the 1930s: Implications for biofuel production. J. Hydrol. 497:110–120. doi:10.1016/j.jhydrol.2013.05.041

Zhang, Y.K., and K.E. Schilling. 2006. Increasing streamflow and baseflow in Mississippi River since the 1940s: Effect of land use change. J. Hydrol. 324:412–422. doi:10.1016/j.jhydrol.2005.09.033